Polarization-dependent x-ray-absorption spectroscopy of single-crystal YNi_2B_2C superconductors

H. von Lips, Z. Hu, C. Grazioli, S.-L. Drechsler, G. Behr, M. Knupfer, M. S. Golden, and J. Fink
Institut für Festkörper- und Werkstofforschung Dresden, D-01171 Dresden, Germany

H. Rosner
Institut für Theoretische Physik, TU Dresden, Dresden, Germany

G. Kaindl
Institut für Experimentalphysik, FU Berlin, Berlin, Germany
(Received 21 May 1999)

Polarization-dependent x-ray-absorption spectroscopy of YNi_2B_2C single crystals is presented for the B 1*s*, C 1*s*, and Ni 2*p* absorption edges. With this technique the electronic structure of the unoccupied states can be examined both in a site and orbitally selective manner. The B 1*s* and C 1*s* absorption spectra reveal a highly anisotropic electronic structure, whereas for the Ni 2*p* edge hardly any anisotropy is found. The experimental data are compared with projected orbital-resolved density of states obtained from local density approximation band-structure calculations. A comparison of experimental and calculated data give good agreement for the B 1*s* and C 1*s* edges. The observed structures at the absorption thresholds of the examined edges support the scenario of a peaked density of states at the Fermi energy leading most probably to the relatively high superconducting transition temperature for this intermetallic compound. [S0163-1829(99)11339-0]

I. INTRODUCTION

The quaternary transition metal borocarbides of general formula RM_2B_2C ($R=Y$, rare earth; $M=$Ni, Pd, Pt) gave with their discovery[1,2] new impetus to the field of intermetallic superconductors, due to their various interesting physical properties which include: (i) the observation of transition temperatures T_c of up to 23 K (for a Y-Pd-B-C compound),[3] which are comparable to those reached in the $A15$ compounds; (ii) their layered structure reminiscent of the high-T_c cuprates; (iii) a peculiar temperature dependence of the upper critical field H_{c2}, which can be explained within a two-band model;[4] (iv) the coexistence of superconductivity and rare earth magnetism.[5]

The crystal structure of RNi_2B_2C has been determined to be body-centered tetragonal with the space group $I4/mmm$,[6] and represents a filled version of the $ThCr_2Si_2$-type structure with additional carbon stabilizing the system. As a result, the Ni-B networks arranged as NiB_4 tetrahedra are separated by a single rock-salt-like RC layer. In other known quaternary borocarbide (-nitride) superconductors such as RNiBC,[2] and $La_3Ni_2B_2N_3$,[7] two RC and three LaN layers are inserted between the Ni-B networks, respectively. The role played by these layers for the superconductivity is still unclear.

For the RM_2B_2C systems, band-structure calculations within the local density approximation (LDA) predict a peak of the electronic density of states (DOS) with the Fermi energy situated close to the peak maximum.[8,9] This has given rise to the assumption that in analogy to the $A15$ compounds, the relatively high superconducting transition temperature is caused by the high DOS at the Fermi energy, $N(E_F)$. In the LDA calculations, the predicted DOS peak at E_F is dominated by Ni 3*d* states, but in fact electronic states from all the constituent atoms contribute. As regards the initial similarities between the RM_2B_2C structure and that of the cuprates, the results of the band-structure calculations indicate dispersive bands in all directions, thus signalling that the electronic structure of these systems is essentially three-dimensional. Accepting the scenario of the DOS peak centered at E_F, as well as a rigid bandlike behavior of the states near E_F, a partial substitution of Ni by Co or Cu should reduce $N(E_F)$. Indeed, transition temperature measurements for $YNi_{2-x}M_xB_2C$ ($M=$Co, Cu) show a decrease in T_c upon doping and from specific heat data a reduction of $N(E_F)$ has been deduced for Co substitution.[10] The question to which extent $N(E_F)$ is an important factor for superconductivity in borocarbides and related systems is, however, still under debate. To understand the pairing mechanism, a detailed knowledge of the electronic structure is essential. Spectroscopic measurements are a direct way to probe the electronic structure and particularly to address the issue of the predicted peak in the DOS at E_F. Spectroscopic investigations of polycrystalline YNi_2B_2C samples have revealed: (i) The absence of a peak at E_F for the occupied states using photoemission spectroscopy (PES).[11,12] (ii) A significant Ni 3*d* contribution to the electronic states of the main valence band and E_F region was shown by resonant PES.[12] (iii) Comparing PES and Auger data, a Ni *d*-*d* on-site Coulomb energy of about 4.4 eV was derived.[13] (iv) Furthermore, a comparison of the integrated Ni $L_{2,3}$ x-ray-absorption spectra of YNi_2B_2C weighted with those of NiO and Ni metal suggests that the 3*d* occupancy is close to that of Ni metal (i.e., $3d^{9.4}$, Ref. 14). Given the Ni 3*d*-derived bandwidth of ca. 6 eV from band-structure calcualtions,[8,9] together with U_{dd} of 4.4 eV and the fact that borocarbides are well away from half-filling, it appears unlikely that electronic correlations will play such a defining role in the rare earth transition metal borocarbides as they do in the cuprate high-T_c superconductors, despite the similar crystal structure. (v) The strongly covalent character responsible for the three-dimensional

electronic structure seen in the band-structure was confirmed by core level excitation measurements using high-energy electron energy-loss spectroscopy (EELS) in transmission.[13] A recent angle resolved photoemission study of cleaved single crystals of YNi_2B_2C has revealed dispersive bands, some of which agree well with the predictions of LDA band-structure calculations. Other observed bands, however, deviate significantly from the LDA predictions and the flat bands giving rise to the DOS peak at E_F were not observed.[15] (vi) X-ray-absorption spectroscopy (XAS) of RNi_2B_2C has not shown any significant changes of the unoccupied electronic structure for R across the rare earth series.[14]

In this paper, we present polarization-dependent XAS measurements on YNi_2B_2C single crystals. This technique allows us to measure the unoccupied electronic states, both site and orbital selectively. We compare our results with orbital-projected partial DOS from LDA band-structure calculations, thus enabling a stringent test of the predictions of one-electron theory. In order to eliminate ambiguity, we have used only single crystals of high purity and good quality, so that no other chemical phases or grain boundary-effects could compromise the results. Our results for YNi_2B_2C are consistent with the existence of a DOS peak centered at E_F.

II. EXPERIMENTAL

The YNi_2B_2C single crystals were grown by the high-temperature floating zone method similar to that described in Ref. 16, except using an inductive heating system.[17] The starting material was stoichiometric polycrystalline YNi_2B_2C melted and formed into rods. Crystals with a diameter of about 4 mm and more than 10 mm long could be obtained in this way. The lattice parameters were determined to be $a = 3.53$ Å and $c = 10.56$ Å and agree with values found in literature.[6] The samples were prepared so as to give a [100] surface, which thus contains the **a** and **c** axes. Smooth surfaces were prepared by either cutting with a diamond knife of an ultramicotrome, polishing with diamond paste (1 μm grain size), or by cleavage. Samples with a cutted surface and a polished surface give essentially the same results.

The XAS experiments were performed at the synchrotron light source BESSY I in Berlin using the SX700-II monochromator,[18] which is operated by the Freie Universität Berlin. The samples were mounted on a rotatable sample holder and were measured at normal incidence with the light polarization vector **E** set parallel to one of the crystallographic **a** or **c** axes. The sample holder was aligned using the reflected zero order light to within an accuracy of better than 1°. The energy resolution of the monochromator was set to 240 meV, 200 meV, and 580 meV for the B 1s, C 1s, and Ni 2p absorption thresholds, respectively. An energy resolution for the B 1s of 180 meV and of 240 meV gave the same spectra and therefore the latter one was chosen to account for a higher photon flux.

In an XAS experiment, an x-ray photon is absorbed in the sample exciting a core electron into an unoccupied state. The obtained excited states can relax by emitting photons or electrons. Therefore, by monitoring either the fluorescence yield (FY) or the total electron yield (TEY), the absorption coefficient for the incident x rays as a function of their energy can be obtained. The fluorescence has an escape depth of the order of 1000 Å, whereas the Auger and secondary electrons giving rise to the TEY signal have a mean free path of the order of 10–100 Å. Consequently, FY is considered as a bulk sensitive method and was therefore used for the XAS measurements presented here. The fluorescence was detected by a solid state Ge detector. Since the initial core states are highly localized, the excitation upon the absorption of the x-ray photon is site selective. Furthermore, dipole selection rules apply. Thus, starting out from the B 1s, C 1s, or Ni 2p core level XAS spectroscopy probes the unoccupied B 2p, C 2p, and Ni 3d/4s electronic states, respectively. With single crystalline samples, the use of polarized light places further restrictions on the final state and in this way one can distinguish between the final orbital states, e.g., for $\mathbf{E}\|\mathbf{a}$ only B $1s \rightarrow B\ 2p_x$ transitions are possible. For comparison, the spectra for $\mathbf{E}\|\mathbf{a}$ and $\mathbf{E}\|\mathbf{c}$ are normalized at energies 70 to 80 eV above the absorption thresholds where the final states are nearly free-electron-like and therefore isotropic. The measured spectra were corrected for the time dependent decrease of the photon flux of the light source using the simultaneously recorded current of the electrons in the storage ring and the energy dependence of the incident flux using TEY spectra taken from a clean gold surface. The energy calibration for the plane grating monochromator was carried out using the Cu $2p_{3/2}$ edge of CuO and the energies of the thresholds of polycrystalline YNi_2B_2C which have been obtained from EELS in transmission.[13] All measurements were performed at room temperature.

III. BAND-STRUCTURE CALCULATION

LDA calculations of the partial DOS of YNi_2B_2C were performed using the linear combination of atomic like orbitals method (LCAO). These scalar relativistic calculations employed a minimal basis set consisting of the Y(5s,5p,4d), Ni(4s,4p,3d), B(2s,2p), and C(2s,2p) orbitals. All energetically lower lying states were treated as core states and a contraction potential has been used at each site to optimize the local basis.[19] The exchange and correlation part was treated within the atomic-spheres approximation, while the Coulomb part of the potential was constructed as a sum of overlapping spherical contributions. Hence, the nonspherical effects of this part determined by the crystal symmetry is taken into account self-consistently. On the other hand, the intra-atomic asphericity is suppressed by azimuthal averaging over the site-charge density during the iteration procedure. The intra-atomic asphericity is only taken into account in the final step of calculating the net density of states (net DOS) of several orbitals.

We define the net DOS as

$$\rho_{net}(\omega) = \frac{1}{N_{\mathbf{k}}} \sum_{\mathbf{k}\nu} \sum_{Lij} |C_{Lij}^{\mathbf{k}\nu}|^2 \delta(\omega - E_{\mathbf{k}\nu}), \qquad (1)$$

where $N_{\mathbf{k}}$ is the number of elementary cells equivalent to the number of $\mathbf{k}$ values and $C_{Lij}^{\mathbf{k}\nu}$ is the coefficient of the wave function $|Lij\rangle$ centered at the atomic site j in the elementary

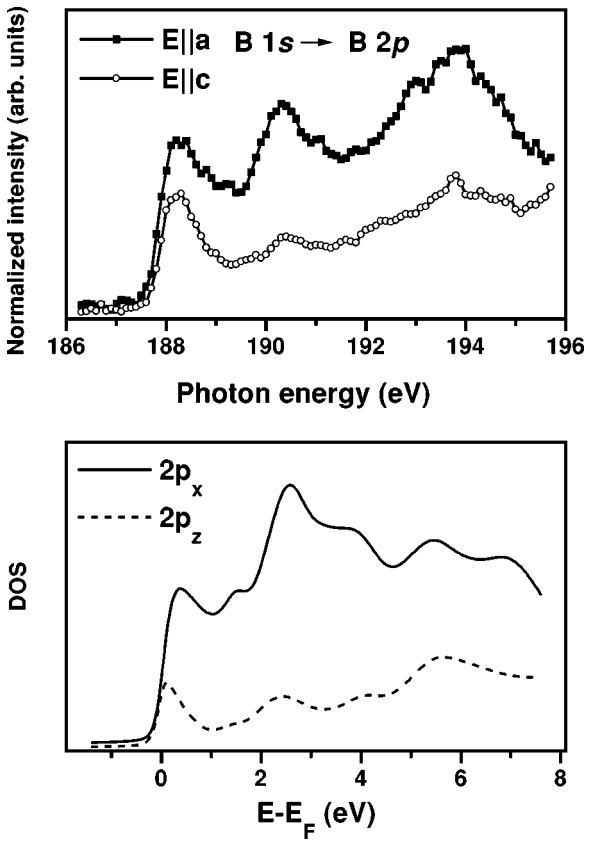

FIG. 1. Boron 1*s* x-ray-absorption spectra of a YNi_2B_2C single crystal for $\mathbf{E}\|\mathbf{a}$ and $\mathbf{E}\|\mathbf{c}$ (upper part); broadened calculated orbital-projected unoccupied DOS for the B $2p_x/2p_z$ orbitals (lower part).

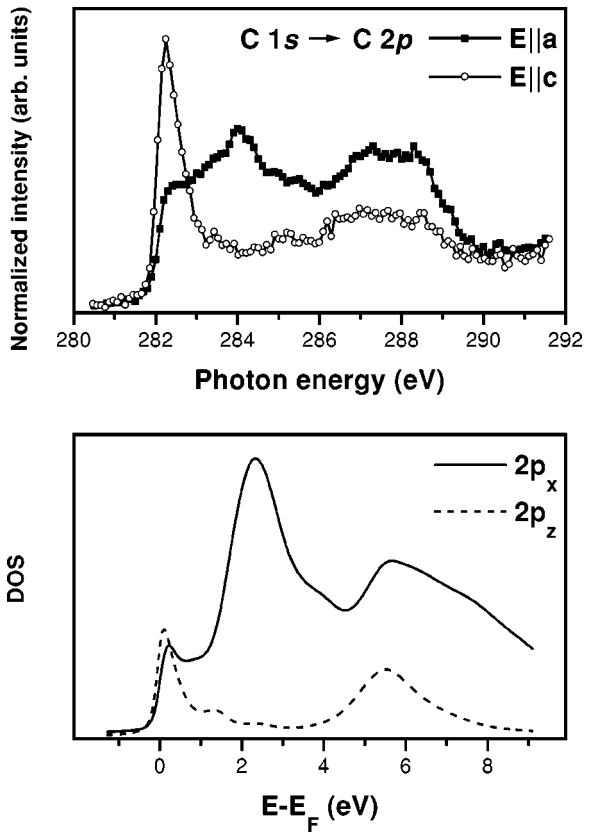

FIG. 2. Carbon 1*s* x-ray-absorption spectra of a YNi_2B_2C single crystal for $\mathbf{E}\|\mathbf{a}$ and $\mathbf{E}\|\mathbf{c}$ (upper part); broadened calculated orbital-projected unoccupied DOS for the C $2p_x/2p_z$ orbitals (lower part).

cell i; $L=\{nlm\}$ with n, l, m denoting the main quantum number, the angular momentum, and the magnetic quantum numbers, respectively.

As the excitations in XAS occur locally, a comparison of the absorption spectra with the calculated net DOS is quite reasonable. The difference between DOS and net DOS consists in the overlap density of states. This difference can be described with a constant factor for all orbitals $|Lij\rangle$ in a given energy interval by an error of less than one percent.[20]

In order to take the quasi-particle and core-hole lifetime effects into account, the partial orbital-projected unoccupied DOS are convoluted with a Lorentzian of FWHM according to $\Gamma+\alpha(E-E_F)$. The atomic 1*s* core-hole lifetime Γ was set equal to the total Auger decay rate of the $2p$ states $r=23.5\,\mathrm{meV}+11.2\,\mathrm{meV}\cdot n_p+10.1\,\mathrm{meV}\cdot n_p(n_p-1)/2$, taken from Ref. 21, where n_p is the occupation of the $2p$ orbitals. From the band-structure calculations, the electron occupancies were determined to about 1 and 2.5 for boron and carbon, respectively, and considering the excited electron, we estimated for the B 1*s* and C 1*s* absorption edges $\Gamma\approx 60\,\mathrm{mV}$ and $\Gamma\approx 110\,\mathrm{meV}$, respectively. For the energy-dependent lifetime of the quasiparticle, $\alpha=0.2$ was chosen.[11] The experimental resolution was accounted for by a convolution with a Gaussian of width equal to the instrumental resolution stated in the experimental section above.

IV. RESULTS AND DISCUSSION

The upper panels of Fig. 1 and Fig. 2 show the B 1*s* and the C 1*s* absorption spectra, respectively, corresponding to transitions into the unoccupied B/C $2p_x$ and B/C $2p_z$ orbitals for polarization along the **a** and **c** axes, respectively. The lower panels of Fig. 1 and Fig. 2 show the appropriate orbital-resolved unoccupied DOS broadened as described above. For comparison, E_F was shifted to the experimental boron 1*s* and carbon 1*s* thresholds located at 187.9 eV and 282.1 eV, respectively.

For the polarization vector **E** parallel to the **a** axis, the B 1*s* excitation spectrum in Fig. 1 shows three main features in the energy range shown: at 188.2 and 190.3 eV and a double structure at 192.9 and 193.9 eV. For $\mathbf{E}\|\mathbf{c}$, one major feature is seen at 188.2 eV and two minor ones at 190.3 and 193.7 eV. All features seen in the XAS spectra can also be found in the corresponding orbital-resolved DOS at about the same relative energy. In the energy range under consideration, the x-ray absorption coefficient is greater for $\mathbf{E}\|\mathbf{a}$ than for $\mathbf{E}\|\mathbf{c}$. This is also evident in the results of our LDA calculations, the relative intensities, however, differ between experiment and theory. Whereas in the XAS data the ratio of the peak at the threshold for $\mathbf{E}\|\mathbf{c}$ and $\mathbf{E}\|\mathbf{a}$ is 2:3, the DOS ratio for the p_z orbital and the p_x orbital at E_F is 1:3.

In the C 1*s* excitation data of Fig. 2 for $\mathbf{E}\|\mathbf{a}$, two peaks at 282.5 eV and 284.0 eV and a broad feature reaching from about 287 to 289 eV are observed. The broad feature is also present in the spectrum with the polarization vector along the **c** axis. The $\mathbf{E}\|\mathbf{c}$ absorption spectrum, however, is dominated by a strong, sharp peak at the absorption onset. The peak ratio at the absorption threshold for $\mathbf{E}\|\mathbf{a}$ and $\mathbf{E}\|\mathbf{c}$ is about 1:2,

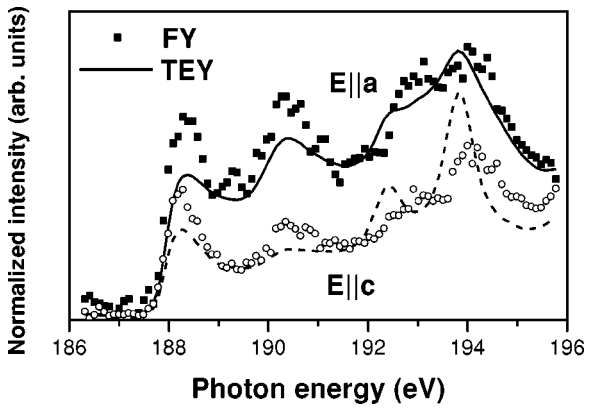

FIG. 3. Boron 1s x-ray-absorption spectra of a cleaved YNi_2B_2C single crystal for $\mathbf{E}\|\mathbf{a}$ and $\mathbf{E}\|\mathbf{c}$ taken with FY (symbols) and TEY (line).

whereas the calculations predict for the DOS at E_F nearly the same intensity for C $2p_x$ and $2p_z$. The relative peak positions for the C 1s absorption spectra are, however, also quite well described by the LDA results.

One reasonable explanation for the difference in the spectral intensity of the XAS and the calculated DOS data for boron and carbon can be found in the short bond length in the **c** direction between the boron and carbon atoms of only ~ 1.55Å,[22] which is even smaller than in hexagonal B_4C (~ 1.64 Å).[23] The strong p_z-orbital overlap of the B $2p$ and C $2p$ states due to the short B-C bond length results in significant Coulomb repulsion between the $2p_z$ electrons, which is not considered in the calculations. Thus the *electron* occupancy of the B $2p_z$ and C $2p_z$ orbital might be significantly lower than is predicted in the LDA calculations.

Nevertheless, we can state that the good overall agreement of the XAS data and band-structure data is a further indication that correlation effects are less important in borocarbides than in the cuprates.

All of the XAS measurements shown in Figs. 1 and 2 have either a steplike or peaked structure at E_F. This is direct evidence that the DOS just above E_F falls off, compatible with the scenario of a peak in the DOS with its maximum near E_F. This confirms the results from specific heat data where a decrease of $N(E_F)$ within a rigid band model is found for substitution of Ni by Co.[10] We note that the Sommerfeld parameter γ and therefore $N(E_F)$ are about twice as large as the LDA calculations predict,[24] pointing to a sizeable renormalization by the electron-phonon interaction, $\gamma \sim N(E_F)(1+\lambda_{el-ph})$. On the other hand, no peak corresponding to a high $N(E_F)$ has been found for the occupied states by photoemission studies.[11,12,15] This might be an indication that the electronic states at the solid-vacuum boundary are quite different and do not support a high value of $N(E_F)$. As the intermetallic borocarbides are strongly covalent, three-dimensional systems cleavage will always lead to the breakage of strong chemical bonds. Possible surface reconstruction may follow to saturate dangling bonds and the DOS could therefore be reduced for the near surface region in comparison to the bulk. This scenario is supported by the XAS data shown in Fig. 3 where the B 1s absorption spectra for a cleaved sample taken simultaneously with the surface and bulk sensitive TEY and FY methods are depicted. While

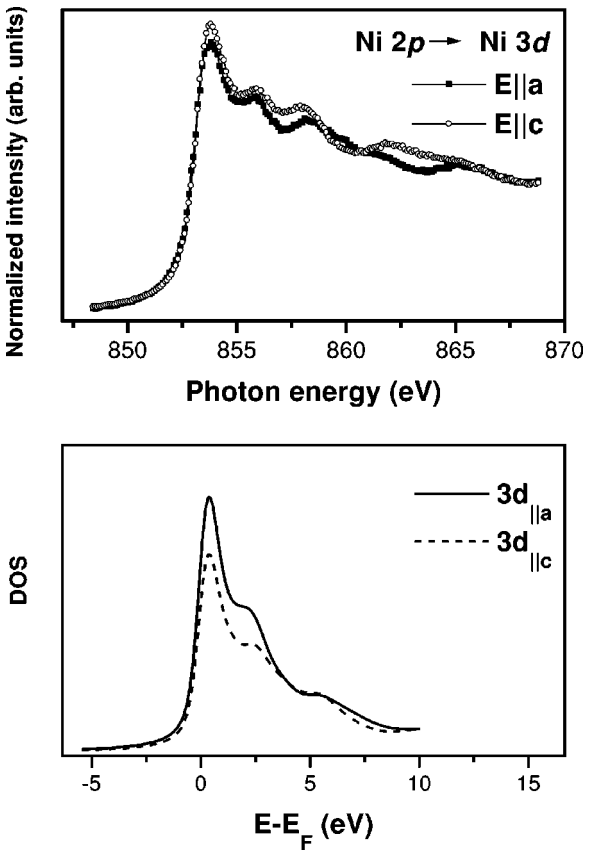

FIG. 4. Nickel $2p$ x-ray-absorption spectra of a YNi_2B_2C single crystal for $\mathbf{E}\|\mathbf{a}$ and $\mathbf{E}\|\mathbf{c}$ (upper part); the spectra are corrected for self-absorption effects (see text); broadened calculated orbital-projected unoccupied DOS for the Ni 3d states where the transition matrix elements are taken into account ($3d_{\|\mathbf{a},c}$ stands for the weighted sum of the orbitals relevant for excitations along the **a** axis or **c** axis).

the FY spectra are—besides statistic effects—identical to those shown in Fig. 1, the TEY spectra are different to the FY spectra. In particular, the peak intensites for both $\mathbf{E}\|\mathbf{a}$ and $\mathbf{E}\|\mathbf{c}$ at the absorption threshold are significantly lower for the TEY spectra than for the FY spectra (the ratio is about 2:3). As PES is even more surface sensitive than TEY, this effect will be even stronger. This, however, strenghtens the conclusions that the peak at the absorption threshold seen with XAS measurements for the unoccupied states is part of the predicted DOS peak situated at E_F.

Figure 4 shows the fluorescence yield XAS spectra at the Ni L_3 edge for $\mathbf{E}\|\mathbf{a}$ and $\mathbf{E}\|\mathbf{c}$. A comparision of the measured FY data with the simultaneously measured TEY data revealed a strong suppression of the fluorescence intensity at the absorption edge. This self-absorption effect is well known in the L-edge XAS of the transition metals. Therefore, a correction for self-absorption according to Ref. 25 was applied. The corrected data in Fig. 4 show main features for both directions at 853.7 eV as well as at about 856 eV and 858 eV. So basically no anisotropy is seen, in contrast to the boron and carbon edges as well as to the LDA predictions for the Ni 3d states when the transition matrix elements are taken into account. This could be ascribed to the significant Coulomb interaction between the Ni $2p$ core hole and the localized excited electron in the 3d state.[26] As a result,

spectral weight is shifted towards the threshold. This so-called white line may dominate the XAS spectra at the threshold. Therefore, a direct comparison with the unoccupied states from band-structure calculations is not possible. The structures seen in the XAS spectra of Fig. 4 starting at about 2 eV above the absorption threshold, however, agree well with LDA calculations.

An analysis of the peak positions relative to the absorption edge for all the spectra shown in Figs. 1, 2, and 4 reveals that they are located at the same relative energies. This reaffirms the earlier observation consistent with strong hybridization among orbitals of all constituent elements and strongly supports the three-dimensional electronic structure, predicted by the LDA calculations.

V. SUMMARY

We examined the unoccupied electronic structure of YNi_2B_2C single crystals using polarization-dependent XAS. A clearly three-dimensional, yet anisotropic electronic structure can be seen. In particular, a strong hybridization between B and C orbitals along the **c** axis is observed. The absorption spectra of B 1*s* and C 1*s* are well described by orbital-projected LDA calculations. This indicates that correlation effects do not dominate the electronic structure in this system. Furthermore, the features in the unoccupied B 2*p* and C 2*p* states at the absorption thresholds are consistent with a DOS peak centered at E_F, as predicted by band-structure calculations. That no peak at E_F could be found for the occupied states with PES can be explained with reconstruction effects at the surface. Our results support the scenario in which the high superconducting transition temperatures in the intermetallic borocarbides are caused by the large $N(E_F)$ value.

ACKNOWLEDGMENTS

This work was supported by the Deutsche Forschungsgemeinschaft within the Sonderforschungsbereich 463 ''Seltenerd-Übergangsmetallverbindungen: Struktur, Magnetismus und Transport.'' Z.H. and R.H. also acknowledge the DFG for support in the framework of the Graduiertenkolleg ''Struktur und Korrelationseffekte in Festkörpern'' at the TU Dresden.

[1] R. Nagarajan, C. Mazumdar, Z. Hossain, S.K. Dhar, K.V. Gopalakrishnan, L.C. Gupta, C. Godart, B.D. Padalia, and R. Vijayaraghavan, Phys. Rev. Lett. **72**, 274 (1994).

[2] R.J. Cava, H. Takagi, H.W. Zandbergen, J.J. Krajewski, W.F. Peck, Jr., T. Siegrist, B. Batlogg, R.B. van Dover, R.J. Felder, K. Mizuhashi, J.O. Lee, H. Eisaki, and S. Uchida, Nature (London) **367**, 252 (1994).

[3] R.J. Cava, H. Takagi, B. Batlogg, H.W. Zandbergen, J.J. Krajewski, W.F. Peck, Jr., R.B. van Dover, R.J. Felder, T. Siegrist, K. Mizuhashi, J.O. Lee, H. Eisaki, S.A. Carter, and S. Uchida, Nature (London) **367**, 146 (1994).

[4] S.V. Shulga, S.-L. Drechsler, G. Fuchs, K.-H. Múller, K. Winzer, M. Heinecke, and K. Krug, Phys. Rev. Lett. **80**, 1730 (1998).

[5] H. Eisaki, H. Takagi, R.J. Cava, B. Batlogg, J.J. Krajewski, W.F. Beck, Jr., K. Mizuhashi, J.O. Lee, and S. Uchida, Phys. Rev. B **50**, 647 (1994).

[6] T. Siegrist, H.W. Zandbergen, J.J. Krajewski, and W.F. Peck, Jr., Nature (London) **367**, 254 (1994); T. Siegrist, R.J. Cava, J.J. Krajewski, and W.F. Peck, Jr., J. Alloys Compd. **216**, 135 (1994).

[7] R.J. Cava, H.W. Zandbergen, B. Batlogg, H. Eisaki, H. Takagi, J.J. Krajewski, W.F. Peck, Jr., E.M. Gyorgy, and S. Uchida, Nature (London) **372**, 245 (1994).

[8] L.F. Mattheiss, Phys. Rev. B **49**, 13 279 (1994).

[9] W.E. Pickett and D.J. Singh, Phys. Rev. Lett. **72**, 3702 (1994).

[10] C.C. Hoellwarth, P. Klavins, and R.N. Shelton, Phys. Rev. B **53**, 2579 (1996).

[11] A. Fujimori, K. Kobayashi, T. Mizokawa, K. Mamiya, A. Sekiyama, H. Eisaki, H. Takagi, S. Uchida, R.J. Cava, J.J. Krajewski, and W.F. Peck, Jr., Phys. Rev. B **50**, 9660 (1994).

[12] M.S. Golden, M. Knupfer, M. Kielwein, M. Buchgeister, J. Fink, D. Teehan, W.E. Pickett, and D.J. Singh, Europhys. Lett. **28**, 369 (1994).

[13] T. Böske, M. Kielwein, M. Knupfer, S.R. Barman, G. Behr, M. Buchgeister, M.S. Golden, J. Fink, D.J. Singh, and W.E. Pickett, Solid State Commun. **99**, 23 (1996).

[14] E. Pellegrin, C.T. Chen, G. Meigs, R.J. Cava, J.J. Krajewski, and W.E. Peck, Jr., Phys. Rev. B **51**, 16 159 (1995).

[15] D.M. Poirier, C.G. Olson, D.W. Lynch, M. Schmidt, and P.C. Canfield (unpublished).

[16] H. Takeya, T. Hirano, and K. Kadowaki, Physica C **256**, 220 (1996).

[17] G. Behr, W. Löser, G. Graw, H. Bitterlich, J. Freudenberger, J. Fink, and L. Schultz, J. Crystal Growth **198/199**, 642 (1999).

[18] M. Domke, T. Mandel, A. Puschmann, C. Xue, D.A. Shirley, G. Kaindl, H. Petersen, and P. Kuske, Rev. Sci. Instrum. **63**, 80 (1992).

[19] H. Eschrig, *Optimized LCAO Method* (Springer-Verlag, Berlin,1989).

[20] H. Rosner, R. Hayn, and J. Schulenburg, Phys. Rev. B **57**, 13 660 (1998).

[21] F. Sette, G.K. Wertheim, Y. Ma, G. Meigs, S. Modesti, and C.T. Chen, Phys. Rev. B **41**, 9766 (1990).

[22] N.M. Hong, H. Michor, M. Vybornov, T. Holubar, P. Hundegger, W. Perthold, G. Hilscher, and P. Rogl, Physica C **227**, 85 (1994).

[23] Calculated from the structure given in H.K. Clark and J.L. Hoard, J. Am. Chem. Soc. **65**, 2115 (1943).

[24] H. Michor, T. Holubar, C. Dusek, and G. Hilscher, Phys. Rev. B **52**, 16 165 (1995).

[25] L. Tröger, D. Arvanitis, K. Baberschke, H. Michaelis, U. Grimm, and E. Zschech, Phys. Rev. B **46**, 3283 (1992).

[26] See, for instance F.M.F. de Groot, J. Electron Spectrosc. Relat. Phenom. **67**, 529 (1994).